Article

Three-Dimensional Hierarchical Hydrotalcite–Silica Sphere Composites as Catalysts for Baeyer–Villiger Oxidation Reactions Using Hydrogen Peroxide

Daniel Cosano *, Dolores Esquivel, Francisco J. Romero-Salguero, César Jiménez-Sanchidrián and José Rafael Ruiz *

Departamento de Química Orgánica, Facultad de Ciencias, Campus de Rabanales,
Instituto Universitario de Investigación en Química Fina y Nanoquímica IUNAN, Universidad de Córdoba,
Edificio Marie Curie, 14071 Córdoba, Spain; q12esmem@uco.es (D.E.); qo2rosaf@uco.es (F.J.R.-S.);
qo1jisac@uco.es (C.J.-S.)

* Correspondence: q92cohid@uco.es (D.C.); qo1ruarj@uco.es (J.R.R.);
Tel.: +34-957-218623 (D.C.); +34-957-218638 (J.R.R.)

Abstract: The development of effective, environmentally friendly catalysts for the Baeyer–Villiger reaction is becoming increasingly important in applied catalysis. In this work, we synthesized a 3D composite consisting of silica spheres coated with Mg/Al hydrotalcite with much better textural properties than its 2D counterparts. In fact, the 3D solid outperformed a 2D-layered hydrotalcite as catalyst in the Baeyer–Villiger reaction of cyclic ketones with H_2O_2/benzonitrile as oxidant. The 3D catalyst provided excellent conversion and selectivity; it was also readily filtered off the reaction mixture. The proposed reaction mechanism, which involves adsorption of the reactants on the hydrotalcite surface, is consistent with the catalytic activity results.

Keywords: three-dimensional hierarchical materials; Baeyer-Villiger reaction; hydrogen peroxide; hydrotalcite; silica

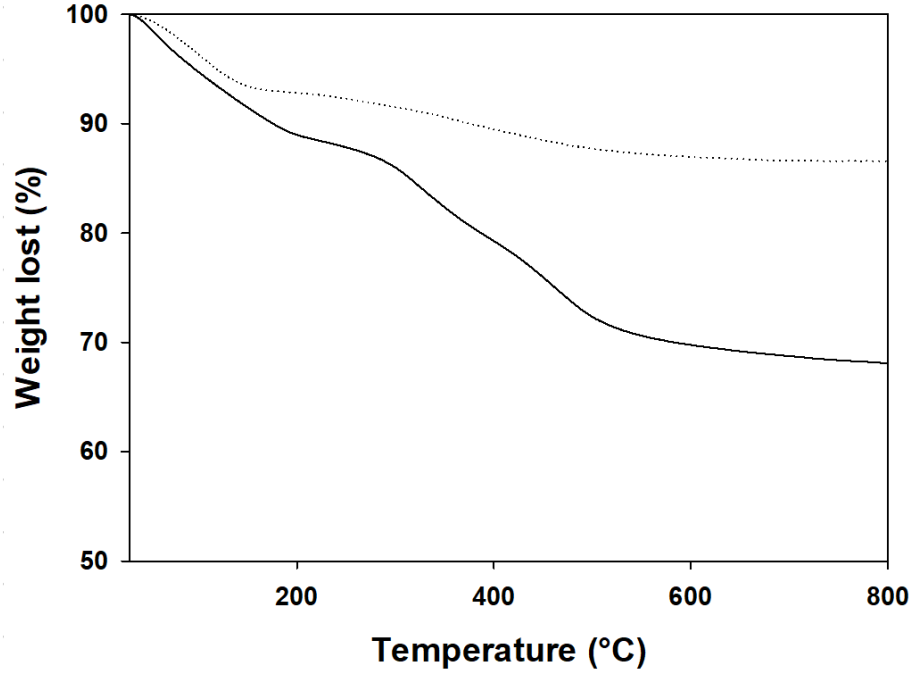

Figure S1. TG profiles for SiO_2@HT (solid line) and SP-SiO_2 (dashed line).

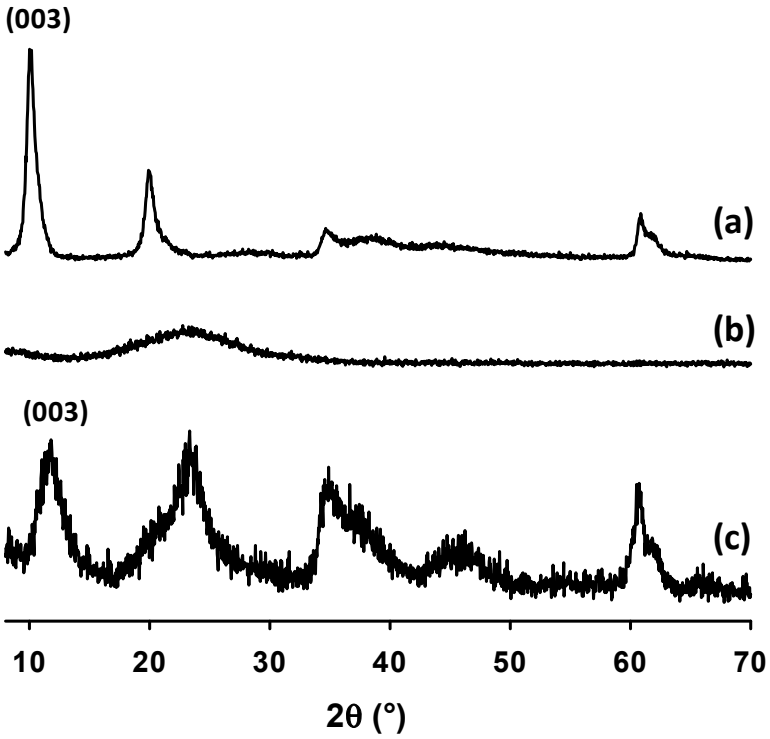

Figure S2. XRD patterns for synthetized solids: HT-2D (a); SiO_2 microspheres; (b) and SiO_2@HT (c).

The XRD pattern (figure S2a) for HT-2D catalyst shows the typical signals for hydrotalcite [1]. For SiO_2 microspheres, the XRD patterns (figure S1b) suggest that these microspheres were amorphous [2]. Finally, the XRD patterns for SiO_2@HT (figure S1c) shows the typical bands for hydrotalcite in addition to a broad halo for silica at 2 values from 15 to 30°. The low intensity of the (003) line is suggestive of little stacking [3]. A comparison of this XRD patterns with those for hydrotalcite reveals that baseline

reflections were shifted to greater 2 values. The shift in baseline reflections to increased 2 values is consistent with a decrease in interlayer distance by effect of a change in interlayer anion. As revealed by the -Raman spectra and explained below, the interlayer anion was carbonate rather than nitrate as in the hydrotalcite.

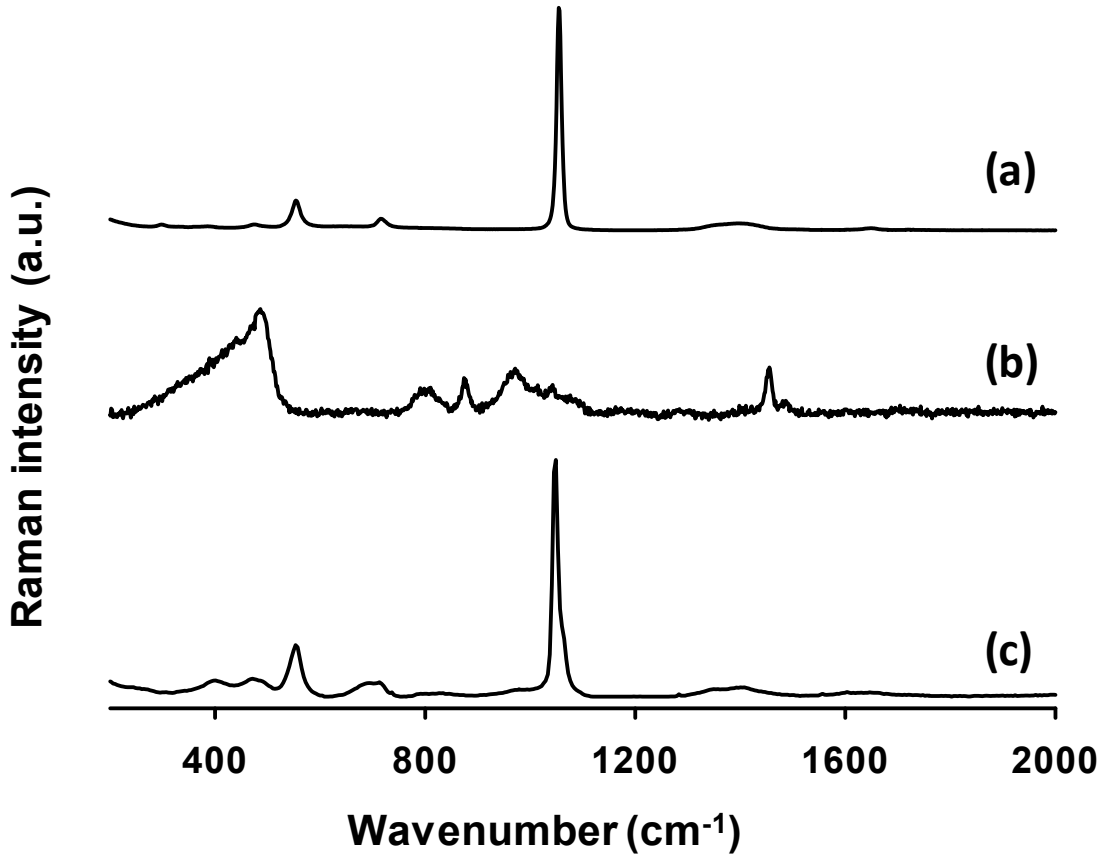

Figure S3. m-Raman spectra for synthetized solids: HT-2D (a); SiO_2 microspheres (b) and SiO_2@HT (c).

Effective intercalation of nitrate anion in HT-2D was confirmed by -Raman spectroscopy. Thus, as can be seen in figure S1a, the presence of the signal at 1055 cm^{-1} and the absence of another at 1060–1070 cm^{-1} typical of carbonate ion indicate that nitrate was the only anion intercalated in the interlayer region. In solid SiO_2@HT (figure S2c) the nitrate signal is also observed, however, a shoulder can be observed, indicative of the presence of carbonate in the interlaminar region, together with nitrate. The presence of this carbonate anion should be related with the sonication step used in this process which was not carried out under inert atmosphere.

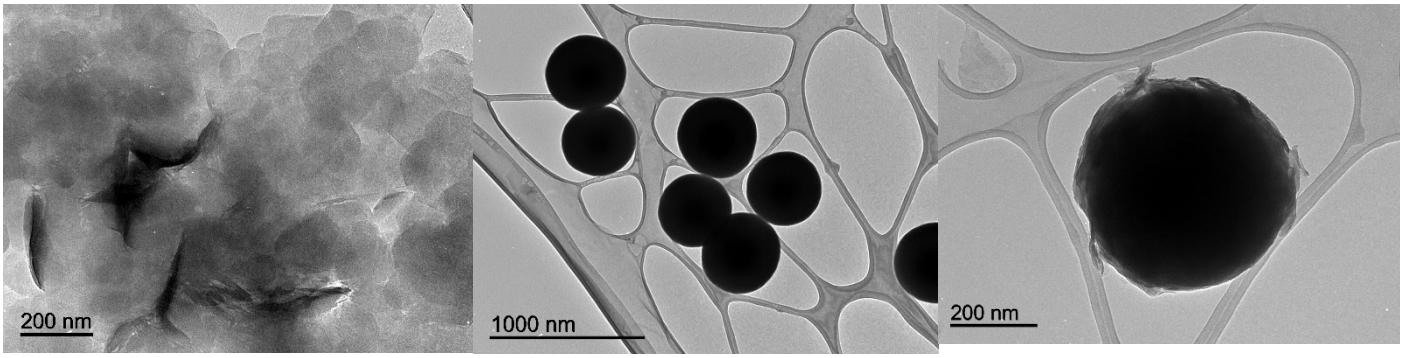

(a) (b) (c)

Figure S4. TEM images for synthetized solids: (a) HT-2D; (b) SiO_2 microspheres and (c) SiO_2@HT.

As can be seen from figure S4a, the solid HT-2D exhibited a roughly hexagonal, plate-like shape in addition to a particle size around 100 nm which is consistent with previously reported values [4]. Figure S4b shows a transmission electron micrograph for the SiO_2 microspheres. As can be seen, they were uniform in diameter (ca. 400 nm). That the coating layers grew around the silica microspheres is confirmed by TEM image of figure S4c.

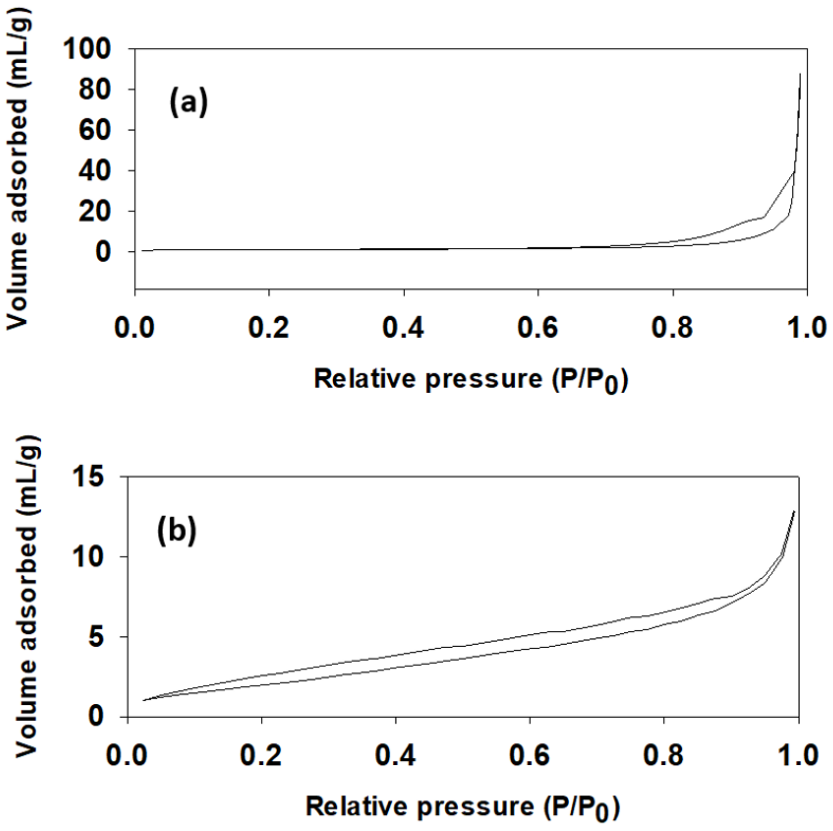

Figure S5. Nitrogen adsorption–desorption isotherm for (a) HT-2D and (b) SP-SiO_2.

Table 1. Comparison of the prepared catalysts with those reported recently.

Catalysts	Reaction conditions	Cyclohexanone conversión (%)	Selectivity (%)	Ref
H-type β-zeolite (Si/Al=39)	30% H_2O_2, acetonitrile, 30°C, 3h	48	52	[5]

Re complexes	30% H_2O_2, 1.2-dichloroethane, 70 °C, 6h	24-57	5-69	[6]
Sn-Beta-HT	30% H_2O_2, 1.4-dioxane, 80 °C, 3h	30	62	[7]
HT-60	30% H_2O_2, acetonitrile, 70 °C, 6h	49	98	[8]
(M)W30	50% H_2O_2, paracetic acid, 50 °C, 5h	64	87	[9]
Mg-Al Hydrotalcites	30% H_2O_2, acetonitrile, 70 °C, 6h	30-40	70-100	[10]
HT-2D	30% H_2O_2, benzonitrile, 90 °C, 6h	39	100	This work
SiO_2@HT	30% H_2O_2, Benzonitrile, 90 °C, 6h	78	100	This Work

References

1. JCPDS Joint committee on powder diffraction standards (JCPDS); 1991;
2. Cavani, F.; Trifirò, F.; Vaccari, A. Hydrotalcite-type anionic clays: Preparation, properties and applications. *Catal. Today* **1991**, *11*, 173–301.
3. Jiang, S.D.; Song, L.; Zeng, W.R.; Huang, Z.Q.; Zhan, J.; Stec, A.A.; Hull, T.R.; Hu, Y.; Hu, W.Z. Self-assembly fabrication of hollow mesoporous Silica@Co-Al Layered Double Hydroxide@Graphene and application in toxic effluents elimination. *ACS Appl. Mater. Interfaces* **2015**, *7*, 8506–8514.
4. Reichle, W.T.; Kang, S.Y.; Everhardt, D.S. The nature of the thermal decomposition of a catalytically active anionic clay mineral. *J. Catal.* **1986**, *101*, 352–359.
5. Taniya, K.; Mori, R.; Okemoto, A.; Horie, T.; Ichihashi, Y.; Nishiyama, S. Role of Al^{3+} species in beta zeolites for Baeyer–Villiger oxidation of cyclic ketones by using H_2O_2 as an environmentally friendly oxidant. *Catal. Today* **2018**, *307*, 293–300.
6. Alegria, E.C.B.A.; Martins, L.M.D.R.S.; Kirillova, M. V.; Pombeiro, A.J.L. Baeyer-Villiger oxidation of ketones catalysed by rhenium complexes bearing N- or oxo-ligands. *Appl. Catal. A Gen.* **2012**, *443–444*, 27–32.
7. Meng, Q.; Liu, J.; Xiong, G.; Liu, X.; Liu, L.; Guo, H. Aerosol-seed-assisted hydrothermal synthesis of Sn-Beta zeolite and its catalytic performance in Baeyer–Villiger oxidation. *Microporous Mesoporous Mater.* **2018**, *266*, 242–251.
8. Olszówka, J.E.; Karcz, R.; Michalik-Zym, A.; Napruszewska, B.D.; Bielańska, E.; Kryściak-Czerwenka, J.; Socha, R.P.; Nattich-Rak, M.; Krzan, M.; Klimek, A.; et al. Effect of grinding on the physico-chemical properties of Mg-Al hydrotalcite and its performance as a catalyst for Baeyer-Villiger oxidation of cyclohexanone. *Catal. Today* **2019**, *333*, 147–153.
9. Han, Y.; Li, S.; Ding, R.; Xu, W.; Zhang, G. Baeyer–Villiger oxidation of cyclohexanone catalyzed by cordierite honeycomb washcoated with Mg–Sn–W composite oxides. *Chinese J. Chem. Eng.* **2019**, *27*, 564–574.
10. Olszówka, J.E.; Karcz, R.; Napruszewska, B.D.; Michalik-Zym, A.; Duraczyńska, D.; Kryściak-Czerwenka, J.; Niecikowska, A.; Bahranowski, K.; Serwicka, E.M. Effect of Mg–Al hydrotalcite crystallinity on catalytic Baeyer-Villiger oxidation of cyclohexanone with H_2O_2/acetonitrile. *Catal. Commun.* **2018**, *107*, 48–52.